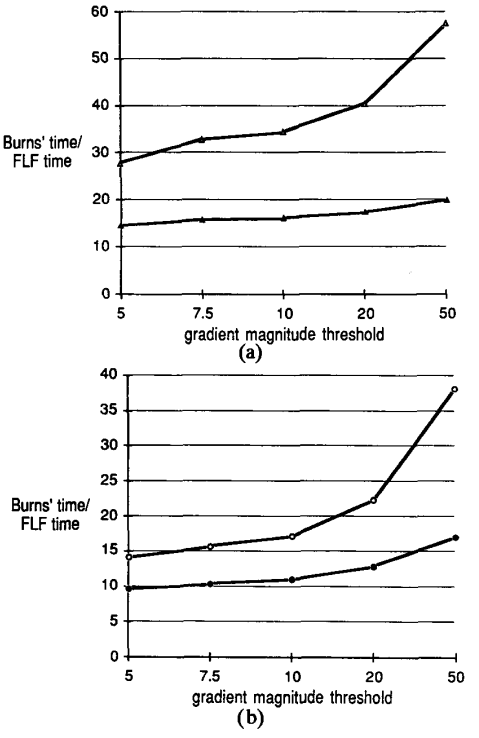

Fig. 6. Burns' versus FLF execution times. (a) FLF using the default 8 buckets; (b) FLF using two buckets tuned ±20°. The bottom curve in each includes the derivative computation time; the upper curve excludes it. For example, in (a) for a gradient magnitude of 5, the FLF time including derivative computation time (the bottom curve) is almost 10 times faster than the Burns algorithm; excluding derivative computation time (the upper curve), it is about 14 times faster.

or parallel processors, using focus-of-attention to define subimages to process, or the use of additional image processing hardware can also be used to approach frame rate performance.

ACKNOWLEDGMEMT

We are indebted to J. B. Burns for his assessments of performance issues and solution techniques. Special thanks are due to R. C. Arkin, M. Boldt, P. Anandan, and INTERNET.

REFERENCES

[1] R. C. Arkin, "Working towards cosmopolitan robots: Intelligent navigation in extended man-made environments," Ph.D. dissertation, Dep. Comput. Inform. Sci., Univ. Massachusetts, Amherst, Sept. 1987.

[2] D. Ballard and C. M. Brown, *Computer Vision.* Englewood Cliffs, NJ: Prentice-Hall, 1982.

[3] J. B. Burns, A. R. Hanson, and E. M. Riseman, "Extracting straight lines," *IEEE Trans. Pattern Anal. Machine Intell.*, vol. PAMI-8, no. 4, pp. 425–455, July 1986.

[4] R. O. Duda and P. E. Hart, *Pattern Recognition and Scene Analysis.* New York: Wiley, 1973.

[5] P. Kahn, L. Kitchen, and E. M. Riseman, "Real-time feature extraction: A fast line finder for vision-guided robot navigation," Dep. Comput. Inform. Sci., Univ. Massachusetts, Amherst, Tech. Rep. 87-57, July 1987.

[6] L. J. Kitchen and J. Malin, "The effect of spatial discretization on the magnitude and direction response of simple differential edge operators on a step edge," *Comput. Vision, Graphics, Image Processing,* vol. 47, pp. 243–258, 1989.

[7] C. Ronse, *Connected Components Algorithms for Binary Images.* New York: Research Studies Press, 1984.

[8] A. Rosenfeld and A. C. Kak, *Digital Picture Processing.* New York: Academic, 1976.

[9] F. M. Vilnrotter, R. Nevatia, and K. E. Price, "Structural analysis of natural textures," *IEEE Trans. Pattern Anal. Machine Intell.*, vol. PAMI-8, no. 1, pp. 76–89, Jan. 1986.

Stereo by Incremental Matching of Contours

Doron Sherman and Shmuel Peleg

***Abstract*—Contours made up of sequences of adjacent edge points are used as primitives in stereo pair matching. Matching contour segments, rather than the traditional epipolar edge points, can greatly reduce possible ambiguity. This is done by reformulating point matching constraints to apply to contour matching, and by introducing a unique incremental matching scheme. Best matched contours are paired first, constraining through neighborhood support their neighboring contours. Examples for the proposed stereo matching scheme are shown, with very few errors, for aerial images of natural terrain.**

***Index Terms*—Curve matching, stereo vision.**

I. INTRODUCTION

Passively sensing three-dimensional structure by means of computational stereo has been addressed both from the biological and computational points of view. Stereo techniques (reviewed in [6]) recover the 3-D location of every point in the scene by bringing its two projections on the pair of images into correspondence and then use 3-D triangulation. Nevertheless, solving this *correspondence problem* is a difficult task.

Biological studies [10], [14], [15] indicate that intensity changes (*edges*) in the image, reflecting physical events in the 3-D world, carry vital information for human stereopsis. Constraints on permissible matches, derived from assumptions about the world and the image formation process, have already been defined for edge-point matching [12]. In this work, the primitive matching elements are contour segments extracted from the images by linking edge points. In order to resolve ambiguous contour candidates effectively, the point matching constraints are reformulated for contour matching.

The matching scheme defines the way in which local and global information interact to yield a set of correspondences between pairs of contours. The scheme developed in this work resembles the relaxation labeling technique [19], [13] in its iterative nature and exploitation of neighborhood relations among potential matches. Matching decisions are made according to local support accumulated from the neighborhood. The strategy is to accept matches in an incremental manner. Most probable candidates (i.e., those having locally highest support) are matched first and are used, with the aid of the reformulated constraints, to introduce restrictions upon other potential matches in their neighborhood.

Manuscript received June 22, 1989; revised April 3, 1990. Recommended for acceptance by J. L. Mundy. Part of this work was performed while S. Peleg was with David Sarnoff Research Center, Princeton, NJ 08543.

The authors are with the Department of Computer Science, the Hebrew University of Jerusalem, 91904 Jerusalem, Israel.

IEEE Log Number 9038387.

As a result, inconsistent candidates are discarded, causing the number of ambiguous candidates to decrease with each additional iteration. The process iterates for the remaining candidates until matches are neither eliminated nor accepted. Thus, the matching algorithm reduces ambiguity until a consistent result, with respect to the locally defined constraints, is reached.

In order to calculate the depth of a scene point from a pair of photographs, the geometric model of the stereo pair and its relation to the scene coordinate system should be known. This can be computed by manually identifying a few corresponding points in the stereo images and providing their 3-D world coordinates [8], [9], [21]. After recovering the complete imaging geometry, the images are corrected (epipolar rectification [3], [5]) to allow scanline to scanline correspondence.

II. Contour Extraction

To extract contour segments, images are first filtered with a recursive gradient operator (Deriche [7]). The filtering operation provides a description of gradient magnitude and direction for each pixel of the image. Edge points are detected by nonmaximal suppression performed on the gradient. A pixel is marked as an edge point if the following conditions hold:

- The edge makes an angle of more than 30° with the x-axis. This requirement prevents using near-horizontal contours which can not be matched accurately.
- The gradient magnitude at the pixel is larger than the gradient at the two neighboring horizontal pixels. This requirement prevents contours from crossing each other.

Marked edge points are then linked into contour segments which are allowed to cross any scanline only once. Each contour segment is traced until an abrupt change in the local edge orientation is encountered. This can help to avoid the linking of nearby edge points belonging to different scene boundaries.

As a consequence, all edge points in one contour segment have the same contrast sign which is used as a contour-related property. In addition, only sufficiently long contour segments are used, as very short contour segments do not contain enough information. The description of each contour includes the following items: length, contrast sign, coordinates of edge points and disparity limits.

III. Contour Matching Constraints

The nature of the stereo correspondence problem allows the formulation of several constraints which are helpful in reducing the ambiguity in the large number of matching alternatives. These constraints are derived from assumptions which are made about the properties of the imaged world, as they are reflected in the stereo imagery. Most constraints were originally formulated for edge points and are modified below in order to apply to contours. It is possible to formulate the constraints directly on the reconstructed surfaces [12], but computation is more efficient when ambiguities are reduced before surface computation.

Shape Similarity: A pair of similar contours, one from each image, is more likely to be the projection of the same physical event in the scene. Arnold and Binford [1] analyzed stereo projections of uniformly distributed line segments in the 3-D world, and found that orientations of corresponding projections tend to be equal. Corresponding contours sharing common scanlines should therefore have similar orientations on the common scanlines [4], [11], [14], [16]. The exact definition of the similarity measure appears in part B of the Appendix.

Contrast Sign: Matched contours must have the same contrast sign.

Disparity Gradient was originally defined for a neighboring pair of point matches. It estimates the local deformation of the disparity field (Pollard, Mayhew, and Frisby [18]). The disparity difference between two pairs of point matches is the absolute difference of disparity of each pair. The cyclopean separation between the two pairs is the distance between their midpoints. The disparity gradient is the ratio between the disparity difference and the cyclopean separation.

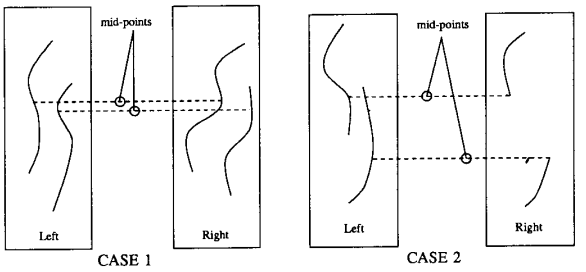

Fig. 1. Two cases of the disparity gradient between contours.

The modified definition of disparity gradient for neighboring pairs of matched contours (Fig. 1) considers the following two cases:

1) The two pairs of contours share at least one common scanline. The disparity gradient is calculated between the edge points on the scanline for which the cyclopean separation is minimal.
2) The two pairs of contours have no scanline in common. The disparity gradient is calculated on the two nearest scanlines. Each pair of edge points lies on a separate scanline.

Following the observation that lengths of corresponding intervals tend to be equal [1], the value of the disparity gradient between two neighboring matches can be bounded. This limit on the permitted disparity gradient is set to the base-to-height ratio, calculated for the acquired stereo pair. The exact definition of the disparity gradient appears in part A of the Appendix.

Figural Continuity: A connected chain of edge points in the image probably represents the projection of a continuous curve in 3-D space (Mayhew and Frisby [15]). Matched contours must therefore form a smooth disparity curve.

Ordering: Given a pair of corresponding scanlines (one on each image), the left-to-right order of matched points along these lines should be preserved (Baker [4], Ohta and Kanade [17]). Such positional reversals may, in fact, occur in certain environments (e.g., transparent objects, wires, etc.) but are seldom encountered in natural outdoor scenes. Since a contour may cross any scanline only once and any two contours may not cross each other, it is sufficient to check for order reversals on one common scanline only.

Uniqueness: The uniqueness constraint (Marr and Poggio [14]) requires that an item on one image may correspond to no more than one item on the other image. For contours, uniqueness is required only on scanlines which are shared by a pair of contours. This allows the matching of split contours caused by imperfect edge detection as shown in Fig. 2, and disallows cases as in Fig. 3.

Epipolar: Rectifying the stereo images enables matching of image points lying on pairs of horizontal lines. As a result, the two-dimensional search required in the general case of image matching, is reduced to a one-dimensional search. This constraint is extended for contour matching by requiring that matchable contours share a minimum number of common (epipolar) scanlines.

IV. Contour Matching Scheme

A. Selecting Potential Matches

Each contour is assigned candidate contours it may match in the other image. The matching process works in both directions, from the left image into the right image and vice versa. Matchable contours obey the following conditions.

Epipolar: Matched contours must have at least eight scanlines in common.

Disparity Range: Measured disparity should be within the allowed limits. (Approximated elevation range is translated into permissible disparities using the known imaging geometry.)

Contrast Sign: Matched contours must have the same sign of contrast.

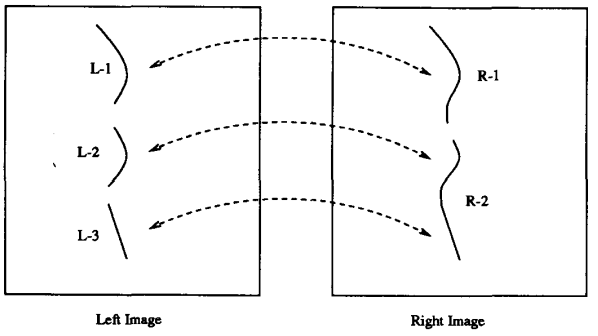

Fig. 2. Unique matching of split contours.

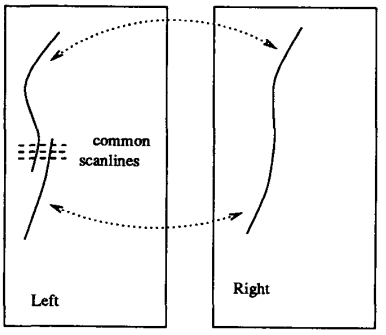

Fig. 3. Violation of the uniqueness constraint.

Local Similarity: Orientations of edge points, lying on common scanlines, must not differ by more than 30 degrees.

After constructing candidate lists for every contour, a measure of shape similarity is calculated for each pair of matchable contours (Appendix, part B).

B. Support Calculation

Neighborhood relations between contours in each image are defined using a grid of windows (Ayache and Faverjon [2]). Neighborhood support is based on the ordering and disparity gradient limit. The latter constraint is quantified (Appendix, part C) so that neighboring matches can influence the relative strengths of each other.

Two attributes are associated with each candidate; one is the support accumulator which gathers scores of the neighbors' support and the similarity values of candidates. The other is the support counter which stores the total number of supporting neighbors. The support for a given candidate (c_i, c_j) is calculated from the neighbors of c_i in the left image as follows.

- For each contour c_h in N^i (neighbors of c_i) do:
  1) For each candidate c_k in L^h (candidates of c_h) do:
     a) Verify that (c_i, c_j) and (c_h, c_k) are ordered properly.
     b) Calculate the disparity gradient for (c_i, c_j) and (c_h, c_k).
     c) If order is reversed or disparity gradient exceeds the limit (base-to-height ratio), then (c_i, c_j) and (c_h, c_k) are inconsistent. If (c_h, c_k) is an accepted match, discard c_j from the candidate list of c_i.
     d) Otherwise, quantify the mutual support between the two pairs (Appendix, part C).
  2) The largest-valued candidate of c_h (denoted by c_k) is chosen to support (c_i, c_j) as follows:
     a) The values of the similarity measure $\mathcal{S}_{hk}$ and the mutual support measure $\mathcal{D}_{ij}^{hk}$ (Appendix, parts B and C) are added to the support accumulator.
     b) The support counter of (c_i, c_j) is incremented by two if (c_h, c_k) is an accepted match, and is incremented by one if (c_h, c_k) is a potential match.

The above steps are repeated for the neighbors of c_j in the right image. Support information from both images is accumulated together (Appendix, part D).

C. Disambiguation Procedure

The disambiguation procedure is an iterative process performing 'Accept' and 'Reject' operations on the set of candidate matches. The procedure starts with the constructed candidate lists of the contours for the left and the right images. Subsequent iterations use neighborhood relations for eliminating inconsistent candidates and for strengthening consistent ones. Each iteration of the process consists of the following steps.

Support calculation: For each contour in the image which has not been assigned a final match, rank the potential matches in its candidate list according to the calculated neighborhood support.

Reject operation: Unsupported candidates are discarded from the candidate lists. This may cause neighboring candidates to become unsupported. The process is repeated recursively until no more unsupported candidates remain.

Accept operation: New accepted matches are obtained by performing the following selections successively on all contours in both images:

1) Select the best candidate in each candidate list.
2) Suppress candidates having less than four supporting neighbors (total support count). Repeat this step again with remaining candidates.
3) Accept candidates as permanent matches if their support count in the neighborhood is maximal.

Validation: Ignore conflicting matches (i.e., those violating the uniqueness or figural continuity constraints) and discard redundant candidates (i.e., those included in a list containing an accepted match).

The above procedure is iterated for both images until candidates are neither discarded nor accepted as permanent matches.

V. Experimental Results

The matching phase provides a sparse set of feature matches, each of which corresponds to a unique 3-D location in the scene. Given a matched pair of edge points, determining the 3-D location is a relatively simple matter of triangulation. Disparity measurements are transformed into ground coordinates, providing a set of irregularly-spaced locations in the 3-D world.

Contours sample the underlying surface shape, particularly at places where real changes occur (e.g., discontinuities in depth) and, hence, they may be used for reconstructing a dense depth map by interpolation. For environments of rolling terrain, a globally smooth surface can be fitted to the boundary conditions established by contour matches with reasonable physical justification. The reconstruction of a two-dimensional function from a sparse set of irregularly-spaced samples is in itself a difficult problem and a subject for extensive research. The method used for performing this task is implemented by an efficient multigrid algorithm (Terzopolous [20]). The final product of the stereo process is a two-dimensional grid containing scene depths at fixed intervals.

The stereo algorithm has been applied to four aerial images of natural terrain. These stereo pairs (512 by 512 pixels in size) have a base-to-height ratio of 0.236 and a mutual overlap of about 80%. The camera model has been derived by identifying manually 18 pairs of corresponding image points, whose 3-D locations in the world are known. Each image is then filtered to provide the gradients (magnitude and direction) which are used by the edge detection and linking procedures to extract contours. The minimal contour length was set to ten pixels. All contours are then transformed into collinear geometry and an initial disparity range which occupies about one fifth of the width of the images is attached to each rectified contour.

TABLE I
NUMBER OF FEATURES AND MATCHING STATISTICS IN IMAGES OF SIZE 512 × 512 AND DISPARITY RANGE 114.

	Image 1	Image 2	Image 3	Image 4
Contours (l, r)	873, 778	979, 1012	881, 847	783, 802
Edge Points (l, r)	12559, 11085	14072, 14436	12624, 12036	11250, 11546
Matched Contours (Errors: #, %)	381 (0, 0%)	503 (2, 0.4%)	310 (1, 0.32%)	326 (2, 0.61%)
Matched Edge Points (Errors: #, %)	5541 (0, 0%)	7203 (19, 0.26%)	4488 (10, 0.22%)	4649 (18, 0.39%)

The iterative matching algorithm is then applied to the stereo set of rectified contours. A grid of windows has been used to partition each image to construct neighborhood relations among contours. The number of iterations needed to resolve the ambiguities and satisfy the stopping conditions (i.e., when additional matches are neither eliminated nor accepted) depends upon the size of the neighbors' lists. For the images used in the experiments, window dimensions of 40 by 40 gave an average list size of 7. With these values, about six to eight iterations of the algorithm were performed until the stopping conditions were met.

Finally, disparities measured on the matched contours were converted into 3-D scene locations, from which a regularly-spaced grid is interpolated. The statistics of matching results for the four stereo pairs are summarized in Table I. The table shows the number of contours and edge points extracted from the stereo imagery and the number (and error percentage) of matched contours and edge points. Examples of two (out of the four) stereo pairs are shown in this correspondence in Figs. 4 and 5. The results of the matching algorithm are presented as follows:

1) An image of the matched contours, registered to the left image of the stereo pair, is displayed in part (c).
2) A contour map of interpolated scene depths, produced from the triangulated 3-D measurements, is shown in part (d). This representation, however, may smooth out rapid depth changes.
3) An isometric view of interpolated depths, coded in a regularly gridded format, is shown in part (e).

VI. CONCLUDING REMARKS

An approach to stereo depth extraction which is primarily concerned with the correspondence problem has been presented. Contours were found to be useful primitives for matching, expressing benefits of the implicit usage of the figural continuity constraint. The other stereo matching constraints, which have been traditionally used for edge points, are modified to handle contours. The suggested matching algorithm is iterative (resembling a discrete relaxation scheme), and utilizes the constraints for obtaining contour correspondences in an incremental manner. The order in which matches are added is determined by their relative strengths. These strengths are estimated dynamically using a measure of support that is gathered from the neighborhood of each potential match.

The performance of the proposed algorithm is shown in examples of stereo pairs from a natural terrain environment. Table I shows that more than one third of the extracted contours are matched. The error rate for those matches is very low (usually less than half percent). The matching algorithm is not very fast in its current implementation, but may run much faster on a multiprocessor machine due to its parallel nature.

In spite of the promising feasibility of the algorithm, additional research has still to be done in order to build a complete stereo system. This research should concentrate on the feature extraction process in order to overcome the imperfections of existing edge detection methods. In addition, a true description of the underlying depth field is dependent upon the interpolation step. Reconstruction of scene surfaces should locate surface boundaries and preserve detected discontinuities.

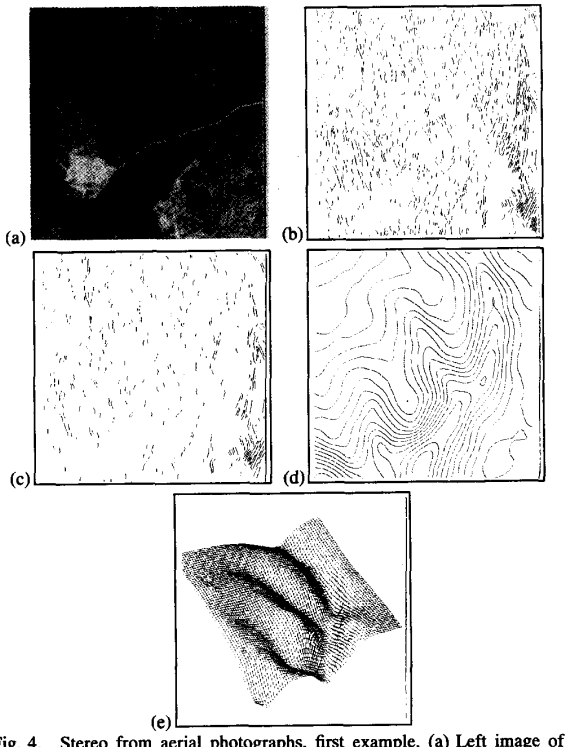

Fig. 4. Stereo from aerial photographs, first example. (a) Left image of a stereo pair. (b) Rectified contours of left image. (c) Matched edges between both images. (d) Contour map of terrain. (e) Isometric plot of interpolated depths.

APPENDIX

A. Disparity Gradient Calculation

Given a point (x_1, y_1) in the left image matched with (x_2, y_1) in the right image and similarly (x_3, y_2) matched with (x_4, y_2), the disparity difference is calculated as

$$\delta = |(x_2 - x_1) - (x_4 - x_3)|, \quad (1)$$

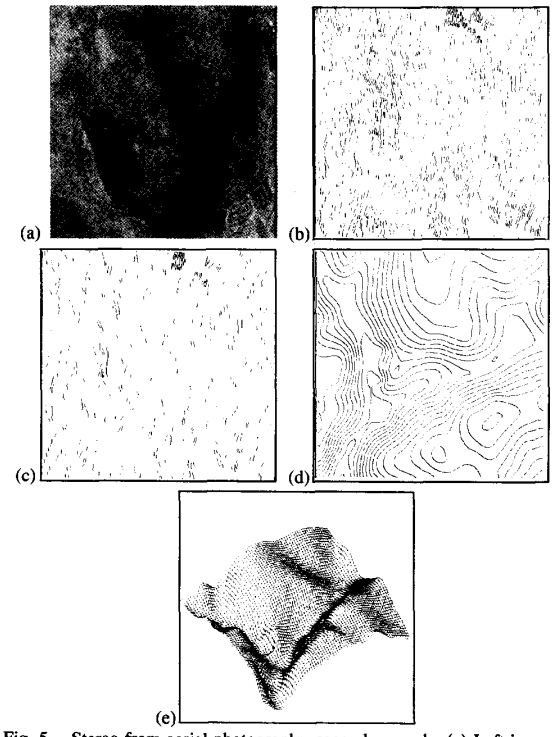

Fig. 5. Stereo from aerial photographs, second example. (a) Left image of a stereo pair. (b) Rectified contours of left image. (c) Matched edges between both images. (d) Contour map of terrain. (e) Isometric plot of interpolated depths.

the cyclopean separation as

$$\gamma = \sqrt{\left[\left(\frac{x_1 + x_2}{2} - \frac{x_3 + x_4}{2}\right)\right]^2 + (y_2 - y_1)^2}, \tag{2}$$

and the disparity gradient as their ratio

$$\xi = \frac{\delta}{\gamma}. \tag{3}$$

B. Contours Similarity Calculation

The local orientation ϕ of an edge point is defined as

$$\phi_{c_i^k} \approx \arctan\left(\frac{X_{c_i^{k+2}} - X_{c_i^{k-2}}}{4}\right),$$

where X is the horizontal image coordinate of an edge point and c_i^k is the edge point of contour c_i lying on scanline k.

The similarity $\mathcal{S}_{ij}$ between potentially matched contours c_i and c_j is defined as

$$\mathcal{S}_{ij} = \sum_{k=k_1}^{k_2} \left(\phi_{\max} - \left|\phi_{c_i^k} - \phi_{c_j^k}\right|\right), \tag{4}$$

where k_1 and k_2 are the upper and lower indexes of the scanlines shared by the pair of contours and $\phi_{\max}$ is arbitrarily set to 30 degrees.

C. Mutual Support Calculation

The mutual support measure $\mathcal{D}_{ij}^{hk}$, between two neighboring pairs of matched contours (c_i, c_j) and (c_h, c_k), is defined as

$$\mathcal{D}_{ij}^{hk} = \frac{\lambda_1}{\delta(c_i, c_j, c_h, c_k)\gamma(c_i, c_j, c_h, c_k) + \lambda_2}, \tag{5}$$

where

- δ is the absolute disparity difference [Equation (1)],
- γ is the cyclopean separation [Equation (2)],
- λ_1 and λ_2 are normalization factors.

D. Total Support Calculation

The accumulated support for a given match (c_i, c_j) is calculated as

$$\text{Support}(c_i, c_j) = \mathcal{S}_{ij} + \sum_{c_h \in N^i} \left(\max_{c_k \in L^h} \left(\mathcal{S}_{hk} + \mathcal{D}_{ij}^{hk}\right)\right) + \sum_{c_k \in N^j} \left(\max_{c_h \in L^k} \left(\mathcal{S}_{hk} + \mathcal{D}_{ij}^{hk}\right)\right), \tag{6}$$

where the notation is identical to that used in (4) and (5).

REFERENCES

[1] R. D. Arnold and T. O. Binford, "Geometric constraints in stereo vision," in *Proc. SPIE Image Processing for Missile Guidance,* vol. 238, San Diego, CA, 1980, pp. 281–292.

[2] N. Ayache and B. Faverjon, "A fast stereovision matcher based on prediction and recursive verification of hypotheses," in *Proc. 3rd Workshop Computer Vision, Representation and Control,* Bellaire, MI, Oct. 1985, pp. 27–37.

[3] N. Ayache and C. Hansen, "Rectification of images for binocular and trinocular stereovision," in *Proc. IEEE Conf. Computer Vision and Pattern Recognition,* 1988, pp. 11–16.

[4] H. H. Baker and T. O. Binford, "Depth from edge and intensity based stereo," in *Proc. 7th Int. Joint Conf. Artificial Intelligence,* Aug. 1981, pp. 631–636.

[5] H. H. Baker, T. O. Binford, and J. Malik, "Progress in stereo mapping," in *Proc. Image Understanding Workshop,* June 1983, pp. 327–335.

[6] S. Barnard and M. Fischler, "Computational stereo," *ACM Comput. Surveys,* vol. 14, no. 4, pp. 553–572, 1982.

[7] R. Deriche, "Using Canny's criteria to derive a recursively implemented optimal edge detector," *Int. J. Comput. Vision,* vol. 1, no. 4, pp. 167–187, 1987.

[8] O. D. Faugeras and G. Toskani, "The calibration problem for stereo," in *Proc. IEEE Conf. Computer Vision and Pattern Recognition,* Miami Beach, FL, June 1986, pp. 15–20.

[9] D. B. Gennery, "Stereo-camera calibration," in *Proc. Image Understanding Workshop,* Los Angeles, CA, Nov. 1979, pp. 101–107.

[10] W. E. L. Grimson, "Aspects of a computational theory of human stereo vision," in *Proc. Image Understanding Workshop,* 1980, pp. 128–149.

[11] ——, "Computational experiments with a feature-based stereo algorithm," *IEEE Trans. Pattern Anal. Machine Intell.,* vol. 7, no. 1, pp. 17–34, Jan. 1985.

[12] W. Hoff and N. Ahuja, "Surfaces from stereo: Integrating feature matching, disparity information, and contour detection," *IEEE Trans. Pattern Anal. Machine Intell.,* vol. 11, no. 2, pp. 121–136, Feb. 1989.

[13] R. A. Hummel and S. W. Zucker, "On the foundations of relaxation labeling processes," *IEEE Trans. Pattern Anal. Machine Intell.,* vol. PAMI-5, no. 3, pp. 267–287, 1983.

[14] D. Marr and T. Poggio, "A computational theory of human stereo vision," in *Proc. Roy. Soc. London,* vol. B204, pp. 301–328, 1979.

[15] J. E. W. Mayhew and J. P. Frisby, "Psychological and computational studies towards a theory of human stereopsis," *Artificial Intell.,* vol. 17, pp. 349–385, 1981.

[16] G. Medioni and R. Nevatia, "Segment-based stereo matching," *Comput. Vision, Graphics, Image Processing,* vol. 31, pp. 2–18, 1985.

[17] Y. Ohta and T. Kanade, "Stereo by intra- and inter-scanline search using dynamic programming," *IEEE Trans. Pattern Anal. Machine Intell.,* vol. PAMI-7, no. 2, pp. 139–154, Mar. 1985.

[18] S. B. Pollard, J. E. W. Mayhew, and J. P. Frisby, "Pmf: A stereo correspondence algorithm using a disparity gradient limit," *Perception,* vol. 14, pp. 449–470, 1985.

[19] A. Rosenfeld, R. A. Hummel, and S. W. Zucker, "Scene labeling by relaxation operations," *IEEE Trans. Syst., Man, Cybern.,* vol. SMC-6, pp. 420–453, June 1976.

[20] D. Terzopolous, "Multiresolution computational processes for visual surface reconstruction," *Comput. Vision, Graphics, Image Processing,* vol. 24, pp. 52–96, 1983.

[21] K. W. Wong, *Manual of Photogrammetry,* 4th ed. Amer. Soc. Photogrammetry, 1980.